Continuous extension of the geometric control method

1996 J. Phys. A: Math. Gen. 29 3545

(http://iopscience.iop.org/0305-4470/29/13/023)

J. Phys. A: Math. Gen. **29** (1996) 3545–3557. Printed in the UK

Continuous extension of the geometric control method

B Sass and Z Toroczkai†

Institute for Theoretical Physics, Eötvös University, Puskin utca 5-7, H-1088 Budapest, Hungary

Received 27 September 1995, in final form 15 February 1996

Abstract. In this paper we give a continuous version (valid for flows) of the geometric control method, introduced in [11] and constructed for mappings on 2D Poincaré sections. This method does not require explicit knowledge of the dynamics, just a rough location of the periodic orbit and a single parameter easily computed from four data points. Applicability in numerical and real experiments is discussed.

1. Introduction and summary

The concept of controlling chaos has attracted recent interest both in theoretical [1–13] and experimental [16–19] areas. The main idea in suppressing chaotic behaviour is to select some desired unstable periodic orbit in the phase space (these orbits fill the phase space densely and serve as backbones for the chaotic behaviour observed [15]) and stabilize it by a *slight* change of the dynamics. A great variety of different stabilizing methods have been constructed (see [6–8] for a review), but most of them require information about the chosen periodic orbit, such as exact location, eigenvalues and eigendirections.

In [11] a self-consistent stabilizing method is given, constructed for mappings on 2D Poincaré sections with the advantage that no information is needed about the periodic orbit, only a rough location of it and the value of a single parameter (k_2) easily computed from four consecutive data points in the vicinity of the periodic orbit. Once the rough location of the desired periodic orbit on the 2D Poincaré section is known (for 'targeting' methods see [11, 14]) together with the parameter k_2, the control is switched on and the unstable (hyperbolic) orbit is reached exponentially fast. The control presented in [11] is done by a *perturbative* change of the dynamics in the vicinity of the desired orbit. The control formula producing the required behaviour is given in terms of the map characterizing the discrete dynamics on the Poincaré section. Therefore the question arises of whether the method could be applied (and how) on continuous systems like the Duffing oscillator, Lorentz system etc or to real experiments.

In this paper we give a continuous version of the same method deriving the perturbative terms to be added to the original system of differential equations (which are not necessarily known in an explicit form) in order to achieve the desired stable behaviour (section 3). Then we show how this is applied in continuous systems by controlling a period-one and a period-two orbit of the Duffing oscillator (section 4). The possibility of experimental applications is also discussed.

† Present address: Department of Physics, Virginia Polytechnic Institute and State University, Blacksburg, VA 24061-0435, USA.

0305-4470/96/133545+13$19.50

2. The geometric control method on 2D Poincaré sections

Before investigating the continuous case (section 3) we would like to give an intuitive and geometric description of the control method presented in [11].

Let us consider a Poincaré section on which the dynamics is characterized by the map $\boldsymbol{F}$ and the linearized vicinity $\mathcal{R}$ of an unstable fixed point (or periodic orbit) $\boldsymbol{R}^*$ to be stabilized. As is emphasized in [11], in order to control (stabilize) the fixed point $\boldsymbol{R}^*$ we only need to know a rough location for it, i.e. the position of the 'target' region $\mathcal{R}$. Nothing about the eigenvalues, eigendirections or accurate localization is needed. The controlling algorithm is constructed in a self-consistent way driving the iteration into the fixed point $\boldsymbol{R}^*$ exponentially fast. Simultaneously we obtain the accurate position, eigenvalues and eigendirections of the fixed point. Although the control formula itself works without any geometric construction, it is called 'geometric' because of the key idea behind its derivation which is illustrated in figure 1. The fixed point is set in the origin in the lower left-hand corner of the figure (not shown in the picture). Let P_0 be some initial point in $\mathcal{R}$, and consider its forward images P_1 and P_2, and one pre-image P_{-1}. These points define three vectors as denoted in figure 1 by $\boldsymbol{v}_1$, $\boldsymbol{u}_1$ and $\boldsymbol{u}_2$. They also define a *level line* having the property that the images and pre-images of any point on this curve lie on the curve itself, see figures 2(*a*) and (*b*). These curves in the case of hyperbolic fixed points are hyperbola-like ones entering $\mathcal{R}$ from the stable direction and exiting along the unstable direction. In the appendix a mathematical definition of these lines is given by deriving their equation in implicit form. Figure 3(*a*) represents the level lines in the case of dissipative dynamics while figure 3(*b*) stands for the conservative case. The fixed point is stabilized only if the sequence of iterations converges into $\boldsymbol{R}^*$. However, because it is an unstable fixed point of the map $\boldsymbol{F}$ the iterations will approach $\boldsymbol{R}^*$ up to a certain extent only (which is the shortest distance between the level line and $\boldsymbol{R}^*$) and then depart from it along the unstable branch of the level line. In order to achieve stable behaviour, it is obvious that the dynamics has to be changed, and such that $\boldsymbol{R}^*$ becomes attractive for the new map. This implies that the new sequence of iterates must 'cross' the level lines of the original map $\boldsymbol{F}$ ending finally

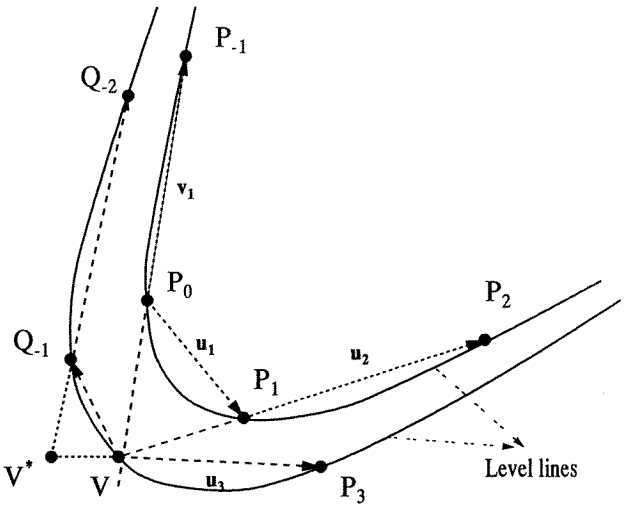

Figure 1. The geometric construction of the controlling algorithm in the geometric control method.

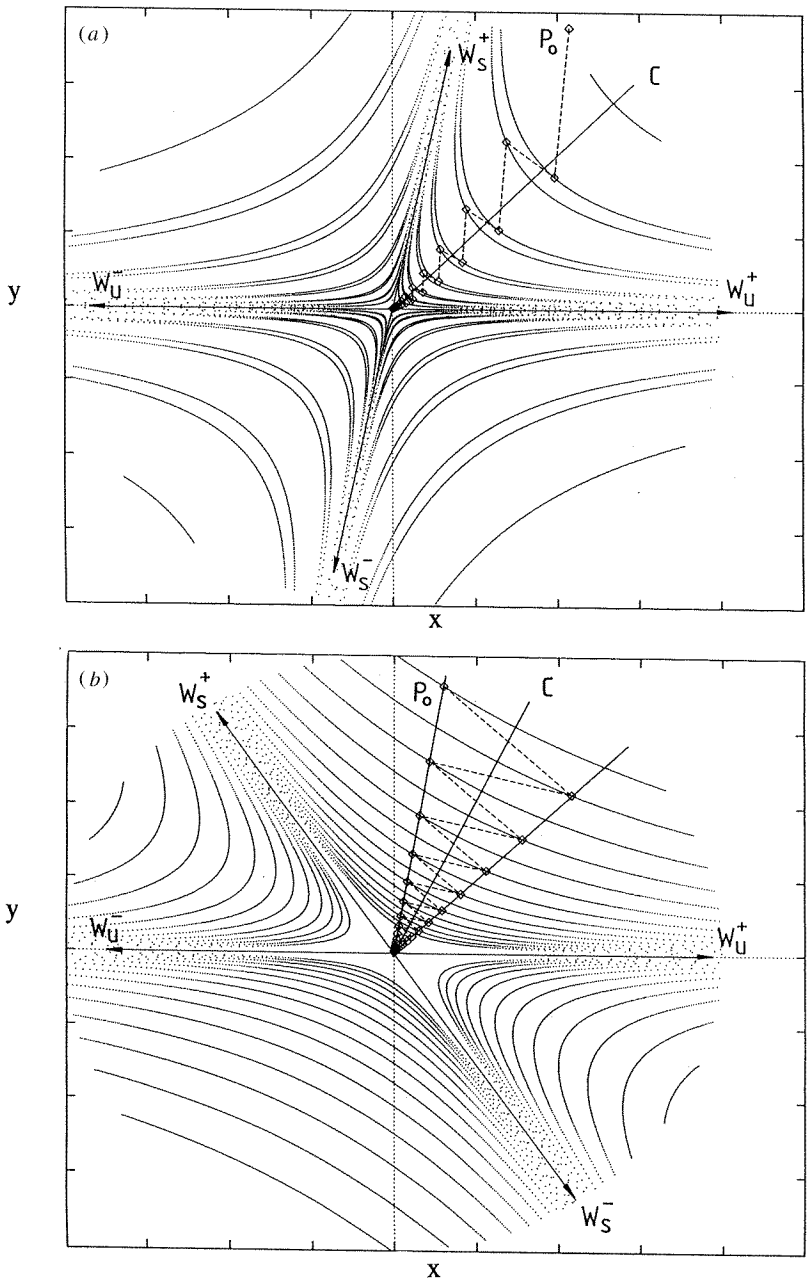

Figure 2. Level lines around a hyperbolic fixed point, for (*a*) dissipative and (*b*) conservative cases. The diamonds show the consecutive steps (the series of V and V^*) of the geometric algorithm for both cases.

in $\boldsymbol{R}^*$ (shown in figures 2(*a*) and (*b*) as the zigzag broken line). (As we will see later, the dynamics is altered in such a way that $\boldsymbol{R}^*$ is a fixed point for the new map, too.) This observation of crossing the level lines of $\boldsymbol{F}$ will be used in the derivation of the new map. We are going to construct geometrically first the sequence of iterates converging into the

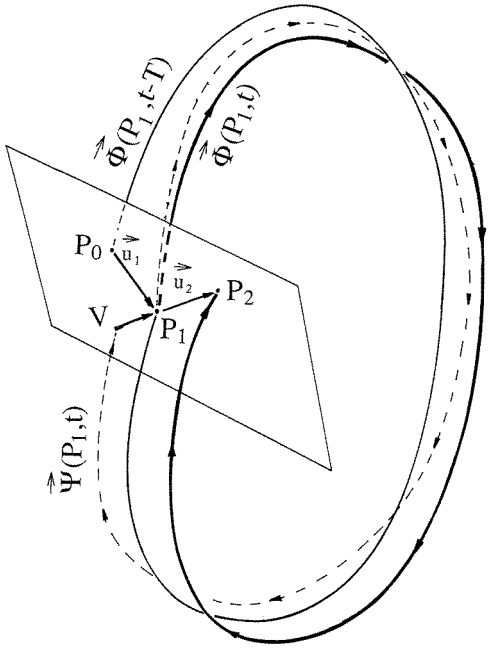

Figure 3. The Poincaré section from figure 1 and the continuous, driven solution Ψ (for Ξ is similar) with endpoint at V on the Poincaré section.

fixed point, and then give the expression (in terms of the iterates of $\boldsymbol{F}$) for the new map. In order to reach a level line closer to $\boldsymbol{R}^*$, let us construct the intersection point of the supports of vectors $\boldsymbol{v}_1$ and $\boldsymbol{u}_2$, denoted by V. Obviously the point V fulfils our claim, i.e. is on a level line closer to the fixed point than the previous one. However, if we continued this process (by successively constructing V) we still would not be able to hit the fixed point, just to approach its unstable manifold closely ($W_u^{\pm}$ in figure 2) and then exit $\mathcal{R}$ along that manifold. This is because when constructing the V we make *one forward step on average* (two forward and one backward) therefore we would leave the fixed point's neighbourhood exponentially fast. In order to perform as many forward as backward steps we need to complete the algorithm by constructing another point V^* as described below.

The point V is mapped in one step into P_3. If we had taken two pre-images of V (shown as Q_{-1} and Q_{-2} in figure 1) then these four points (including V and P_3) would determine the intersection point V^* in the same manner as V was determined by the set of four points P_{-1}, P_0, P_1 and P_2. (However, as will see, it is not necessary to take the backward images which in practical situations is generally not possible.) Let us denote by $\boldsymbol{X}_M$ the position vector of the point M in a coordinate system with the origin in $\boldsymbol{R}^*$.

The position of V^* is related in the same way to the vector $\boldsymbol{u}_3 = \boldsymbol{X}_{P_3} - \boldsymbol{X}_V$ (defined by the points V and P_3) as V is related to $\boldsymbol{u}_2 = \boldsymbol{X}_{P_2} - \boldsymbol{X}_{P_1}$ (see figure 1):

$$\boldsymbol{X}_V = \boldsymbol{X}_{P_1} + k_2[\boldsymbol{X}_{P_1} - \boldsymbol{X}_{P_2}] \tag{1}$$

$$\boldsymbol{X}_{V^*} = \boldsymbol{X}_V + k_2[\boldsymbol{X}_V - \boldsymbol{X}_{P_3}] \tag{2}$$

where k_2 is the ratio between the lengths of the collinear vectors $\boldsymbol{X}_{P_1} - \boldsymbol{X}_V$ and $\boldsymbol{u}_2$ (or $\boldsymbol{X}_{V^*} - \boldsymbol{X}_V$ and $\boldsymbol{u}_3$). In [11] is shown that k_2 is actually the inverse value of the trace of the linearized dynamics around $\boldsymbol{R}^*$, and is easily found from four consecutive data points

in $\mathcal{R}$:

$$k_2 = \frac{|\boldsymbol{u}_1 \times \boldsymbol{v}_1|}{|\boldsymbol{u}_2 \times \boldsymbol{v}_1|}\,. \tag{3}$$

The process starting from P_0 and ending in V^* is called one iteration step of the geometric method. In the next step take V^* as a starting point (as P_0) and repeat the procedure again and again. The point V is just an intermediate construction point, the series of iterates for the new map being the V^* (started from P_0). It is also obvious that the geometrical construction of V^* involves three forward iterates (the points P_1, P_2 starting from P_0 and P_3 starting from V) and three backward ones (P_{-1} from P_0 and Q_{-1}, Q_{-2} from V) therefore *on average* zero steps are made. This assures that the sequence of V^* does not leave $\mathcal{R}$ once it is started from there. After a few steps one can reach the origin (which is $\boldsymbol{R}^*$) with very high accuracy because of the fact that the iteration from point P_0 to V^* (or the new map) has both eigenvalues smaller than unity in absolute value, i.e. the fixed point for this map is an attractive one (for a proof, see [11]). In the general case the accurate position of $\boldsymbol{R}^*$ might be unknown, as well as the linearized dynamics around it (i.e. the explicit expression of the linearized $\boldsymbol{F}$ in $\mathcal{R}$). It is assumed that we can only generate (with a computer or an experimental device) the image (output) of an input point. Therefore, the control formula has to be expressed in terms of the full map $\boldsymbol{F}$. This can easily be given on the basis of expressions (1) and (2). It reads as

$$\boldsymbol{R}_{n+1} = \boldsymbol{E}^2(\boldsymbol{F}(\boldsymbol{R}_n)) \qquad n = 0, 1, 2, \ldots \tag{4}$$

where

$$\boldsymbol{E}(\boldsymbol{R}) = \boldsymbol{R} + k_2[\boldsymbol{R} - \boldsymbol{F}(\boldsymbol{R})]\,. \tag{5}$$

$\boldsymbol{R}_0$ is (the position vector of) a starting point in $\mathcal{R}$ (as P_0), then $\boldsymbol{F}(\boldsymbol{R}_0)$ corresponds to P_1 and $\boldsymbol{F}(\boldsymbol{F}(\boldsymbol{R}_0)$ to P_2 in figure 1. $\boldsymbol{E}$ then makes a shift to V and another application of it takes the iterate to V^*. Using instead of $\boldsymbol{F}$ the map $\boldsymbol{E}^2 \circ \boldsymbol{F}$, the fixed point $\boldsymbol{R}^*$ becomes stable.

Observe that the function $\boldsymbol{E}$ in (5) differs from the identity function by a *perturbative* term only. And this term $|\boldsymbol{R} - \boldsymbol{F}(\boldsymbol{R})|$ becomes smaller and smaller when approaching $\boldsymbol{R}^*$. Thus the control is achieved by a *slight* change of the dynamics in the target region. When one constructs the continuous version of (4) this property will be kept. Again, we emphasize that (4) and (5) work without any geometrical interpretation, the latter being presented only as the originating idea for them.

3. Control formula for three-dimensional flows

The stabilizing algorithm given in [11] is useful when one can easily construct the image points in some Poincaré section together with the modified map of the control formula (4). If the map $\boldsymbol{F}$ is constructed from a system of continuous differential equations (such as, for example, the Duffing oscillator, the Röessler system etc) then the interesting question naturally arises of what is a corresponding system of continuous differential equations for the modified map (4) of the control formula? Another reason for answering this question is continuity. Observe that the control (4), (5) acts *in* the Poincaré section. This would mean that in practice we have to wait until the trajectory arrives on this plain and then *suddenly* apply the action of $\boldsymbol{E}$. In practical situations this might be hard to accomplish. The iterates through $\boldsymbol{F}$ are generated 'continuously' in the space outside the Poincaré section but for $\boldsymbol{E}$ this is no longer true. If the Poincaré section presented in figure 1 is taken somewhere in the three-dimensional space of some set of ODEs, then we have to give the (continuous)

part of the trajectory between the points P_1 and V (the mapping $\boldsymbol{E}$) *outside* the Poincaré section. This means solving the problem of driving the continuous solution started at time $t = 0$ from the point P_0 into the point P_1 (at $t = T$), then into V at (at $t = 2T$), and finally into V^* (at time $t = 3T$) (see figure 3). This continuous driving is performed by adding *perturbative* terms to the original system of differential equations.

In the following we give the derivation of these additional terms. Assume that the map $\boldsymbol{F}$ is generated by a system of autonomous, ordinary differential equations (ODEs):

$$\dot{\boldsymbol{Y}} = \boldsymbol{D}(\boldsymbol{Y}) \,. \tag{6}$$

Let $\boldsymbol{Y}_0(t)$ denote a periodic solution to (6) with period T:

$$\boldsymbol{Y}_0(t + T) = \boldsymbol{Y}_0(t) \tag{7}$$

and let us consider a thin tube $\mathcal{T}$ around the closed curve $\boldsymbol{Y}_0(t)$ so that the flow is linearized inside $\mathcal{T}$, i.e. equation (6) is approximated by

$$\dot{\boldsymbol{X}} = \boldsymbol{A}\boldsymbol{X} \tag{8}$$

where

$$\boldsymbol{X}(t) = \boldsymbol{Y}(t) - \boldsymbol{Y}_0(t) \tag{9}$$

and

$$\boldsymbol{A} = \left.\frac{\partial \mathbf{D}}{\partial \boldsymbol{Y}}\right|_{\boldsymbol{Y}=\boldsymbol{Y}_0(t)} \tag{10}$$

is the derivative matrix of $\boldsymbol{D}$ (time dependent through $\boldsymbol{Y}_0(t)$). Here $\boldsymbol{X}(t)$ is analogous to $\boldsymbol{X}_M$ from the previous section. Imagine a Poincaré section as the plane perpendicular to the curve given by the solution $\boldsymbol{Y}_0(t)$ at time $t = 0$, see figure 3. The intersection point $\boldsymbol{Y}_0(0)$ is identified with the fixed point $\boldsymbol{R}^*$ from section 2. Moreover, the same local coordinate system can be considered with the origin in $\boldsymbol{R}^*$. $\mathcal{R}$ is just the domain on the plane cut out by the tube $\mathcal{T}$. We shall denote by $\Phi(P_0, t)$ a solution of (8) with initial condition P_0:

$$\dot{\Phi}(P_0, t) = \boldsymbol{A}(t)\Phi(P_0, t) \qquad \Phi(P_0, 0) = \boldsymbol{X}_{P_0} \,. \tag{11}$$

More correct would be the notation $\Phi(\boldsymbol{X}_{P_0}, t)$ because Φ as a function depends on the coordinates (or position vector) of the point P_0 and not on the point itself, but because this will not create confusion, however, we use the simpler notation. Obviously the relation

$$\Phi(P_0, t) = \Phi(P_1, t - T) \tag{12}$$

holds. It just means that the trajectory started at time t from P_0 and arrived in P_1 after time T; it is equivalent to the trajectory started from P_1 at the later time $t - T$. Observe that $\Phi(P_0, T) = \boldsymbol{X}_{P_1}$. To drive the trajectory continuously from P_1 to V one has to change (8) such that at $t = T$ the desired relation (1) is valid. Let us denote the continuous solution of the perturbed system of ODEs starting from P_1 and ending after one period in V by $\boldsymbol{\Psi}(P_1, t)$. Thus

$$\boldsymbol{\Psi}(P_1, 0) = \boldsymbol{X}_{P_1} \qquad \boldsymbol{\Psi}(P_1, T) = \boldsymbol{X}_V \,. \tag{13}$$

Our requirements are only (1) and (13) and the restriction that Ψ be inside the tube $\mathcal{T}$ at any time $0 < t < T$.

We give a possible solution, but one has to emphasize that this is not unique. Infinitely many curves can be constructed with the specified limit conditions inside $\mathcal{T}$. Consider the following form for the solution Ψ:

$$\boldsymbol{\Psi}(P_1, t) = \Phi(P_0, t) + \alpha(t)\left[\Phi(P_0, t) - \Phi(P_1, t)\right] \,. \tag{14}$$

The continuity requirement and the limit conditions (1), (13) fix the value of the function $\alpha(t)$ at the endpoints:

$$\alpha(0) = -1 \qquad \alpha(T) = k_2 \tag{15}$$

(for $t = T$ we get back (1)). From equation (14) one can express $\Phi(P_1, t)$ as

$$\Phi(P_1, t) = \frac{1+\alpha(t)}{\alpha(t)}\Phi(P_0, t) - \frac{1}{\alpha(t)}\Psi(P_1, t)\,. \tag{16}$$

In order to find the system of ODEs having the solution $\boldsymbol{\Psi}$, take the derivative of (14) with respect to time:

$$\dot{\boldsymbol{\Psi}}(P_1, t) = \dot{\Phi}(P_0, t) + \alpha(t)\left[\dot{\Phi}(P_0, t) - \dot{\Phi}(P_1, t)\right] + \dot{\alpha}(t)\left[\Phi(P_0, t) - \Phi(P_1, t)\right]\,. \tag{17}$$

From equations (11) and (12): $\dot{\Phi}(P_1, t) = \boldsymbol{A}(t+T)\Phi(P_1, t)$. Then using (16) and the fact that the matrix $\boldsymbol{A}$ is periodic, i.e. $\boldsymbol{A}(t \pm T) = \boldsymbol{A}(t)$ (because the system is autonomous, $\boldsymbol{A}(t)$ depends on t only through $\boldsymbol{Y}_0(t)$ which is periodic) we obtain

$$\dot{\boldsymbol{\Psi}}(P_1, t) = \boldsymbol{A}(t)\boldsymbol{\Psi}(P_1, t) + \frac{\dot{\alpha}(t)}{\alpha(t)}\left[\boldsymbol{\Psi}(P_1, t) - \Phi(P_0, t)\right]. \tag{18}$$

The second expression on the right-hand side of (18) gives the required additional (perturbative) term. The divergence of this term at $\alpha = 0$ is only apparent because at this value the difference in the rectangular brackets also vanishes, such that the perturbative force disappears (from equation (14) it follows that when $\alpha = 0$: $\boldsymbol{\Psi}(P_1, t) = \Phi(P_0, t)$). For the moment we leave the function α undetermined and return to its specification later.

Let us now drive the solution from the point V in the Poincaré section to the point V^*, see figure 1. For this, consider the modified solution (denoted by $\boldsymbol{\Xi}$) in the form

$$\boldsymbol{\Xi}(V, t) = \boldsymbol{\Psi}(P_1, t) + \beta(t)\left[\boldsymbol{\Psi}(P_1, t) - \Phi(V, t)\right]. \tag{19}$$

Again, we are searching for the system of ODEs having the solution (19) with initial and endpoints in V and V^*, respectively. Proceeding analogously as before, we find

$$\begin{aligned}\dot{\boldsymbol{\Xi}}(V, t) = \boldsymbol{A}(t)\boldsymbol{\Xi}(V, t) &+ \frac{\dot{\beta}(t)}{\beta(t)}\left[\boldsymbol{\Xi}(V, t) - \boldsymbol{\Psi}(P_1, t)\right] \\ &+ \left[1 + \beta(t)\right]\frac{\dot{\alpha}(t)}{\alpha(t)}\left[\boldsymbol{\Psi}(P_1, t) - \Phi(P_0, t)\right].\end{aligned} \tag{20}$$

From equation (19) the boundary conditions (see also equations (1) and (2)):

$$\boldsymbol{\Xi}(V, 0) = \boldsymbol{X}_V = \boldsymbol{X}_{P_1} + \beta(0)[\boldsymbol{X}_{P_1} - \boldsymbol{X}_V] \tag{21}$$

and

$$\boldsymbol{\Xi}(V, T) = \boldsymbol{X}_{V^*} = \boldsymbol{X}_V + \beta(T)[\boldsymbol{X}_V - \boldsymbol{X}_{P_3}] \tag{22}$$

yield

$$\beta(0) = -1 \qquad \beta(T) = k_2\,. \tag{23}$$

Comparing (23) with (15) we can make the following identification:

$$\alpha(t) \equiv \beta(t)\,. \tag{24}$$

With this identification the expression of (20) takes the simpler form

$$\dot{\boldsymbol{\Xi}}(V, t) = \boldsymbol{A}(t)\boldsymbol{\Xi}(V, t) + \frac{\dot{\alpha}(t)}{\alpha(t)}\left[\boldsymbol{\Xi}(V, t) - \Phi(P_0, t)\right] + \dot{\alpha}(t)\left[\boldsymbol{\Psi}(P_1, t) - \Phi(P_0, t)\right]. \tag{25}$$

Being arrived in V^*, the whole procedure can then be repeated again and again, and the series of V and V^* will converge exponentially to the fixed point.

It is worth rewriting the formulae above in terms of the original system of differential equations $\boldsymbol{D}$. This can be done rather easily by using (7), (9) and (10). From P_0 to P_1 we have (see equation (11)):

$$\dot{\boldsymbol{Y}}(t) = \boldsymbol{D}(\boldsymbol{Y}(t)) \qquad t \in [0, T] \qquad \boldsymbol{Y}(0) = \boldsymbol{Y}_0(0) + \boldsymbol{X}_{P_0}\,. \tag{26}$$

From P_1 to V (see equation (18)):

$$\dot{\boldsymbol{S}}(t) = \boldsymbol{D}(\boldsymbol{S}(t)) + \frac{\dot{\alpha}}{\alpha}[\boldsymbol{S}(t) - \boldsymbol{Y}(t)] \qquad t \in [0, T] \qquad \boldsymbol{S}(0) = \boldsymbol{Y}(T) \tag{27}$$

and from V to V^* (see equation (25)):

$$\dot{\boldsymbol{Q}}(t) = \boldsymbol{D}(\boldsymbol{Q}(t)) + \frac{\dot{\alpha}}{\alpha}[\boldsymbol{Q}(t) - \boldsymbol{Y}(t)] + \dot{\alpha}[\boldsymbol{S}(t) - \boldsymbol{Y}(t)]$$
$$t \in [0, T] \qquad \boldsymbol{Q}(0) = \boldsymbol{S}(T)\,. \tag{28}$$
$$\tag{29}$$

The $\boldsymbol{S}(t)$ and $\boldsymbol{Q}(t)$ are the corresponding solutions in the global coordinate system (the one in which (6) is written) to the solutions $\boldsymbol{\Psi}(t)$ of (18) and $\boldsymbol{\Xi}(t)$ of (25), respectively. As we can see, the above equations have to be solved in the order (26), (27), (29). After solving (26) take as starting point $\boldsymbol{Y}(T)$ for (27) then solve it in the time interval $t \in [0, T]$, etc. Then when $t = T$ in the last equation, take $\boldsymbol{Q}(T)$ as a starting position for the first one again, and repeat the cycle. The above equations are certainly not in the most convenient form, but they can be put together in a single system of ODEs:

$$\dot{\boldsymbol{Z}}(t) = \boldsymbol{D}(\boldsymbol{Z}(t)) + \omega_1(t)\frac{\dot{\gamma}}{\gamma}[\boldsymbol{Z}(t) - \boldsymbol{Z}(t-T)] + \omega_2(t)\dot{\gamma}\frac{1+\gamma}{\gamma}[\boldsymbol{Z}(t-T) - \boldsymbol{Z}(t-2T)]$$
$$t \in [0, \infty) \qquad \boldsymbol{Z}(0) = \boldsymbol{Y}_0(0) + \boldsymbol{X}_{P_0} \tag{30}$$

where ω_1, ω_2 and γ are the functions

$$\omega_1(t) = \Theta\left[\frac{1}{2} + \cos\left[\left(\frac{t}{T} + 1\right)\frac{2\pi}{3}\right]\right]$$
$$\omega_2(t) = \Theta\left[-\frac{1}{2} - \cos\left[-\left(\frac{t}{T} - 1\right)\frac{2\pi}{3}\right]\right] \tag{31}$$
$$\gamma = \alpha\left(T\left\{\frac{t}{T}\right\}\right)$$

with $\Theta(x)$ as the Heaviside function ($\Theta(x) = 1$ if $x > 0$, otherwise $\Theta(x) = 0$), and $\{x\}$ is the fractional part of the real number x. ω_1 and ω_2 are two square waves presented in figure 4. It is easy to see that when $3k \leqslant \{t/3T\} \leqslant 3k + 1$ ($k = 0, 1, 2, \ldots$) then (30) reduces to (26), ($\omega_1 = \omega_2 = 0$) when $3k + 1 \leqslant \{t/3T\} \leqslant 3k + 2$ then (30) reduces to (27) ($\omega_1 = 1$, $\omega_2 = 0$), and for $3k + 2 \leqslant \{t/3T\} < 3(k + 1)$, (29) is recovered ($\omega_1 = \omega_2 = 1$).

For the function α, besides the boundary conditions (15) the only restriction is that the solutions $\boldsymbol{\Psi}$ and $\boldsymbol{\Xi}$ be inside the linearized domain, i.e. tube $\mathcal{T}$. It is easy to see that this is fulfilled by the simplest, i.e. linear form of α:

$$\alpha(t) = \frac{1 + k_2}{T}t - 1\,. \tag{32}$$

In order to perform the control we need to keep track the trajectory for a time interval equal to $2T$ in the past (see equations (30)). It gives the information necessary to determine the future of the trajectory which is on the desired periodic orbit.

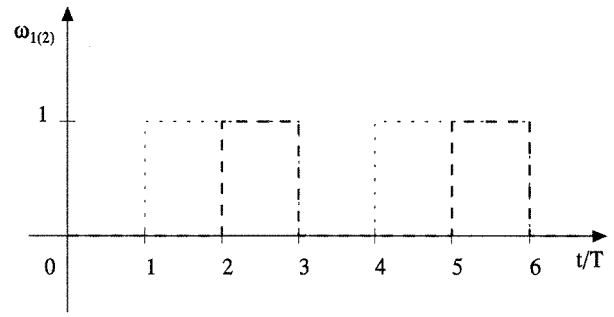

Figure 4. The ω_1 (thin broken line) and ω_2 (thick broken line) functions.

4. An example. Applicability of the control method

To illustrate the applicability of the ideas above let us take the Duffing oscillator [8, 9]:

$$\boldsymbol{D}: \quad \dot{x} = y \qquad \dot{y} = -x^3 + ay + b\cos t \tag{33}$$

at parameter values $a = 0.3$ and $b = 39$. Obviously, equation (33) is a non-autonomous, time-periodic system, but it is equivalent to a three-dimensional time-independent system after introducing a third coordinate z and a third equation $\dot{z} = 1$ with the initial condition for z: $z(0) = 0$. Figure 5 shows the chaotic trajectory started from $(0, 0)$ at $t = 0$ and stopped at $t = 20T$ (here $T = 2\pi$). In figures 6(a) and (b) one can see two stabilized (using equation (30)), (a) a period-one and (b) a period-two orbit. Figure 6(c) shows the

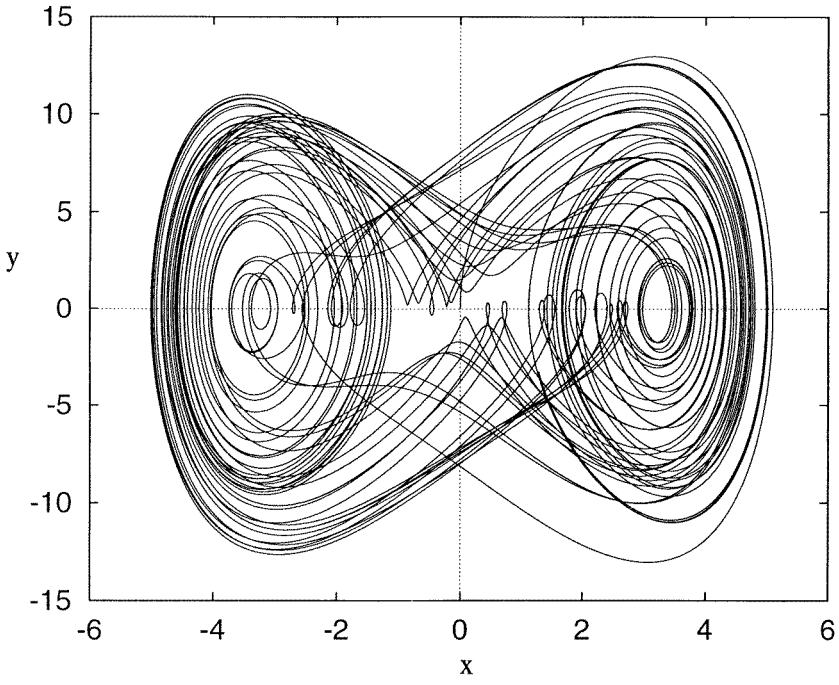

Figure 5. Chaotic trajectory of the Duffing oscillator (equation (30)) started from point (0, 0) at $t = 0$ and stopped at $t = 40\pi$.

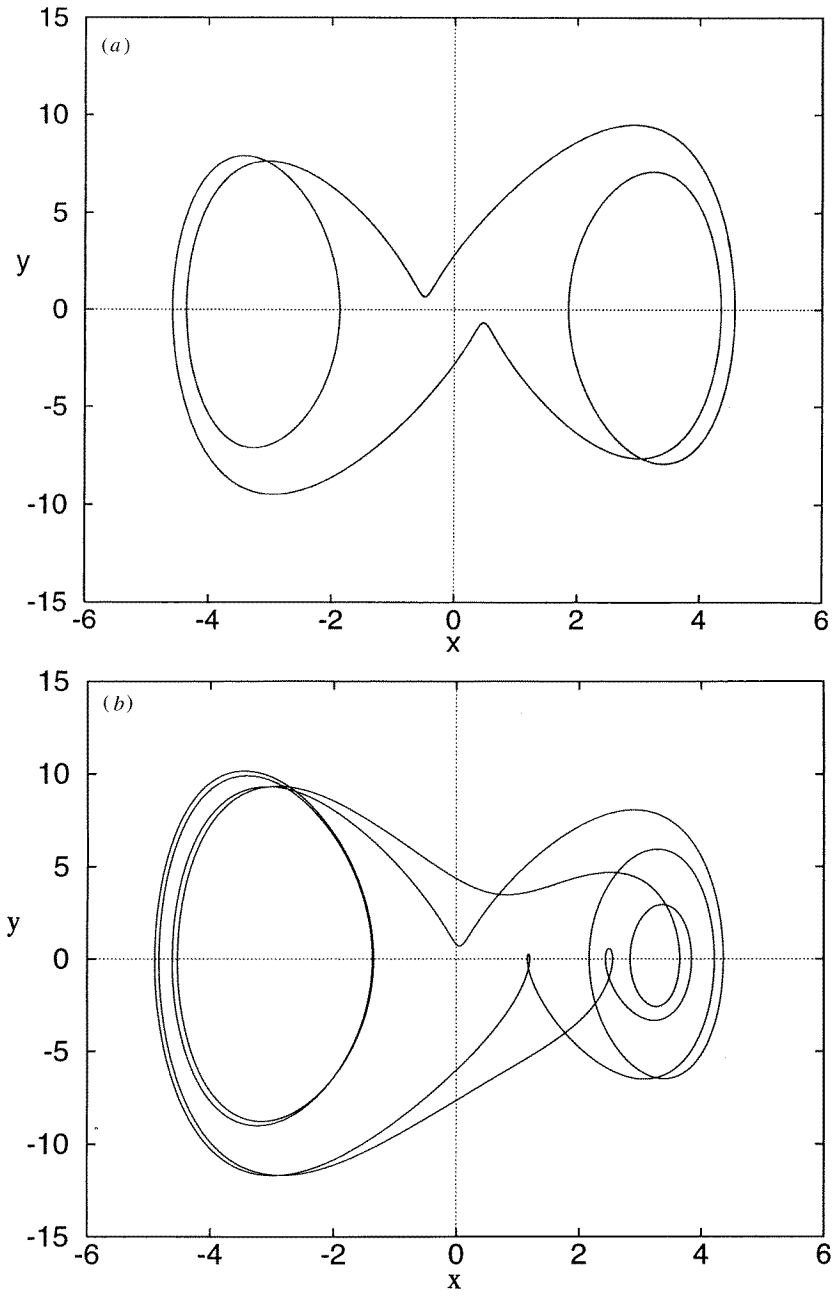

Figure 6. A stabilized, period-one orbit of the Duffing oscillator (*a*) with coordinates $x = 1.893$, $y = -1.422\,88$ on the Poincaré section, and (*b*) a period-two orbit with coordinates $x = 2.164\,01$, $y = 0.021\,76$.

series of successive V^* in the Poincaré section (for the period-one orbit from figure 6(*a*)), exponentially converging to the fixed point.

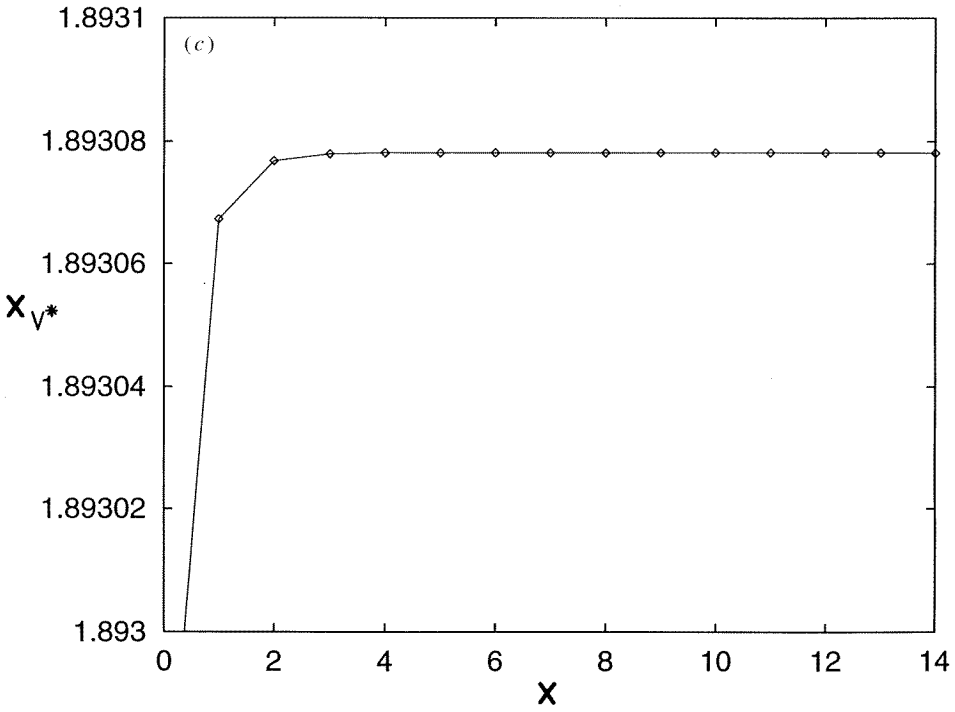

Figure 6. (Continued.) (*c*) The exponentially converging series of successive V^* in the Poincaré section, for the period-one orbit.

From the expression for the controlled system of ODEs in (30) one can see that the terms added are perturbative and dissipative. These correspond to the addition of dissipative (and perturbative) forces to the system which stabilize the desired periodic orbit as long as these forces are present in the system. Because these forces are making use of the present and the previous states of the system only (besides the $\omega_{1(2)}$ and γ simple functions), we believe that there are experiments in which with properly designed devices these damping forces can be created and used for control.

Numerically, the method can be used successfully anytime and as an example we can mention the hydrodynamical two-dimensional advection problems. The surface dynamics of a single, advected particle even in a time-periodic velocity field can be strongly chaotic [20]. Therefore the equations of motion are similar in structure to the equations for the Duffing oscillator, but usually they are much more complicated and their form cannot be given explicitly in terms of analytic functions. However, numerically (30) presents no problems.

5. Conclusions

In the present paper we gave a continuous extension valid for three-dimensional flows of the geometric method [11]. The advantage of the method is the fact that only a previous rough localization of the periodic orbit is needed, the orbit's period T and a single parameter k_2 which can easily be computed using formula (3) from four data points. By 'rough' we mean a deviation from the real orbit not larger than the domain in which the flow can be linearized. It is also required that these four consecutive points be all in this domain (on

a previously chosen Poincaré section). No knowledge is needed about the eigenvalues and eigenvectors of the periodic orbit. The perturbative velocity field which controls the system is given by the two extra terms in (30). These contain *memory* terms, using previous states of the system as feedback and, therefore, a continuous monitoring of the states is needed. However, we do not have to keep track of the trajectory for a time interval longer than twice the orbit's period.

Also note that the control is not achieved by tuning a certain parameter of the system (which in some cases might not be available) but by adding the above-mentioned perturbative memory-type dissipative forces.

Acknowledgments

The authors are indebted for useful discussions with T Tél, C Jung, Á Péntek, S Manservisi and G Korniss. One of the authors (ZT) is grateful to the Hungarian Science Foundation for partial support of this work under grants no OTKA F4286, OTKA F17166 and to the Foundation for Hungarian Higher Education and Research.

Appendix. Implicit equation for level lines

Although it is not directly related to the application of the control formulae (30) and (26)–(29) themselves, it is interesting to give a defining equation for these level lines.

Let us then consider that the map in the linear neighbourhood of the fixed point considered in the origin and characterized on the Poincaré section by the 2×2 matrix $\boldsymbol{L}$:

$$\boldsymbol{L} = \begin{pmatrix} a & b \\ c & d \end{pmatrix}.$$

Then the nth image of an initial point $\boldsymbol{r}_0$ through the iteration will be given by

$$\boldsymbol{r}_n = \boldsymbol{L}^n \boldsymbol{r}_0 \,. \tag{A1}$$

Our goal is to find an equation for the curve determined by the set of points $\boldsymbol{r}_n$. Let $\lambda_{1(2)}$ be the eigenvalues of the matrix $\boldsymbol{L}$ above. Then two eigenvectors belonging to these eigenvalues will be given by

$$\text{for } \lambda_1: \quad \begin{pmatrix} 1 \\ \dfrac{\lambda_1 - a}{b} \end{pmatrix} \qquad \text{and for } \lambda_2: \quad \begin{pmatrix} 1 \\ \dfrac{\lambda_2 - a}{b} \end{pmatrix}. \tag{A2}$$

Observe that $m_1 \equiv (\lambda_1 - a)/b$ and $m_2 \equiv (\lambda_2 - a)/b$ are the slopes of the two eigendirections. By using a similarity transformation:

$$\boldsymbol{L} = \boldsymbol{U}^{-1} \boldsymbol{\Omega} \boldsymbol{U} \tag{A3}$$

with

$$\boldsymbol{\Omega} = \begin{pmatrix} \lambda_1 & 0 \\ 0 & \lambda_2 \end{pmatrix} \qquad \boldsymbol{U} = \frac{1}{m_2 - m_1} \begin{pmatrix} m_2 & -1 \\ -m_1 & 1 \end{pmatrix} \qquad \text{and} \qquad \boldsymbol{U}^{-1} = \begin{pmatrix} 1 & 1 \\ m_1 & m_2 \end{pmatrix}. \tag{A4}$$

Therefore (A1) reads as

$$\boldsymbol{U} \boldsymbol{r}_n = \boldsymbol{\Omega}^n \boldsymbol{U} \boldsymbol{r}_0 \tag{A5}$$

or explicitly

$$m_2 x_n - y_n = \lambda_1^n (m_2 x_0 - y_0) \qquad -m_1 x_n + y_n = \lambda_2^n (-m_1 x_0 + y_0) \tag{A6}$$

where (x_n, y_n) are the coordinates of the point with position vector $\boldsymbol{r}_n$. By eliminating n from the two equations above, is found:

$$\ln|\lambda_2|\ln|m_2x_n - y_n| - \ln|\lambda_1|\ln|-m_1x_n + y_n| = \ln|\lambda_2|\ln|m_2x_0 - y_0| - \ln|\lambda_1|\ln|-m_1x_0 + y_0| = \text{constant} \equiv K \qquad \forall n\,. \tag{A7}$$

Therefore, the level lines are equivalent to the family of curves

$$\frac{|m_2x - y|^{\ln|\lambda_2|}}{|-m_1x + y|^{\ln|\lambda_1|}} = \mathrm{e}^K \tag{A8}$$

being valid in all four quadrants. If the dynamics is conservative, i.e. $|\lambda_1\lambda_2| = 1$ the equation above simplifies to $|(m_2x - y)(-m_1x + y)| =$ constant, which is the equation for a regular hyperbola. Figures 3(*a*) and (*b*) display the level lines for both dissipative and conservative cases.

References

[1] Ott E, Grebogi C and Yorke J A 1990 *Chaos: Proc. of a Soviet–American Conf.* (New York: American Institute of Physics); 1990 *Phys. Rev. Lett.* **64** 1196

[2] Tél T 1991 *J. Phys. A: Math. Gen.* **24** L1359; 1993 *Int. J. Bif. Chaos* **3** 757
Kovács Z, Szabó K G and Tél T 1993 Controlling chaos on fractal basin boundaries *Proc. Dynamical Systems Conf. (London)* to appear

[3] Pyragas K 1992 *Phys. Lett.* **170A** 421

[4] Dressler U and Nitsche G1992 *Phys. Rev. Lett.* **68** 1

[5] Lai Y-C, Ding M and Grebogi C 1993 *Phys. Rev.* E **47** 86

[6] Abarbanel H D, Brown R, Sidorovich J J and Tsimring L Sh 1993 *Rev. Mod. Phys.* **65** 1331

[7] Romeiras F J, Grebogi C, Ott E and Dayawansa W P 1992 *Physica* **58D** 165

[8] Chen G and Dong X 1993 *Int. J. Bif. Chaos* **6** 1363

[9] Chen G and Dong X 1993 *IEEE Trans. Circuits Syst.* **CS-40**
Chen G 1993 *IEEE Trans. Circuits Syst.* **CS-40** 829

[10] Romeiras F J, Ott E, Grebogi C and Dayawansa W P 1991 Controlling chaotic dynamical systems *Proc. American Control Conf.* (New York: IEEE Press) p 1112

[11] Toroczkai Z 1994 *Phys. Lett.* **190A** 71

[12] Kadtke J, Péntek Á and Pedrizzetti G 1995 *Phys. Lett.* **204A** 108

[13] Xu D and Bishop S R 1996 *Phys. Lett.* **210A** 273

[14] Shinbrot T, Grebogi C, Ott E and Yorke J A 1992 *Phys. Lett.* **169A** 349

[15] Cvitanović P 1991 *Physica* **51D** 138

[16] Ditto W L, Rauseo S N and Spano M L 1990 *Phys. Rev. Lett.* **65** 3211
Hunt E R 1991 *Phys. Rev. Lett.* **67** 1953
Singer J, Wang Y-Z and Bau Haim H 1991 *Phys. Rev. Lett.* **66** 1123
Azevedo A and Rezende S 1991 *Phys. Rev. Lett.* **66** 1342
Hunt E R 1992 *Phys. Rev. Lett.* **68** 1259

[17] Reyl C, Flepp L, Badii R and Brun E 1993 *Phys. Rev.* E **47** 267

[18] Petrov V, Gáspár V, Masere J and Showalter K 1993 *Nature* **361** 240

[19] Rollins R W, Parmananda P and Sherard P 1993 *Phys. Rev.* E **47** R780
Peng B, Petrov V and Showalter K 1991 *J. Phys. Chem.* **95** 4957; 1992 *Physica* **188A** 210
Petrov V, Peng B and Showalter K 1992 *J. Chem. Phys.* **96** 7506

[20] Ottino J M 1989 *The Kinematics of Mixing: Streching, Chaos and Transport* (Cambridge: Cambridge University Press)
Péntek Á, Toroczkai Z, Tél T, Grebogi C and Yorke J A 1995 *Phys. Rev.* E **51** 4076 (and references therein)